AFRL-RY-WP-TR-2014-0152

METASTABLE PACKAGING FOR TRANSIENT ELECTRONICS

Jeffrey S. Moore, Scott R. White, Nancy R. Sottos, John A. Rogers, Bora Inci, Joshua A. Kaitz, Seung-Kyun Kang, Olivia P. Lee, Hector Lopez Hernandez, and Chan Woo Park

University of Illinois

SEPTEMBER 2014
Final Report

AIR FORCE RESEARCH LABORATORY
SENSORS DIRECTORATE
WRIGHT-PATTERSON AIR FORCE BASE, OH 45433-7320
AIR FORCE MATERIEL COMMAND
UNITED STATES AIR FORCE

NOTICE AND SIGNATURE PAGE

Using Government drawings, specifications, or other data included in this document for any purpose other than Government procurement does not in any way obligate the U.S. Government. The fact that the Government formulated or supplied the drawings, specifications, or other data does not license the holder or any other person or corporation; or convey any rights or permission to manufacture, use, or sell any patented invention that may relate to them.

This report is the result of contracted fundamental research deemed exempt from public affairs security and policy review in accordance with SAF/AQR memorandum dated 10 Dec 08 and AFRL/CA policy clarification memorandum dated 16 Jan 09. This report is available to the general public, including foreign nationals.

Copies may be obtained from the Defense Technical Information Center (DTIC) (http://www.dtic.mil).

AFRL-RY-WP-TR-2014-0152 HAS BEEN REVIEWED AND IS APPROVED FOR PUBLICATION IN ACCORDANCE WITH ASSIGNED DISTRIBUTION STATEMENT.

//Signature//

CARRIE M. BARTSCH, Program Manager
Devices for Sensing Branch
Aerospace Components & Subsystems Division

//Signature//

ROSS W. DETTMER, Chief
Devices for Sensing Branch
Aerospace Components & Subsystems Division

//Signature//

BRADLEY D. CHRISTIANSEN, Lt Col, USAF
Deputy Division Chief
Aerospace Components & Subsystems Division
Sensors Directorate

This report is published in the interest of scientific and technical information exchange, and its publication does not constitute the Government's approval or disapproval of its ideas or findings.

*Disseminated copies will show "//Signature//" stamped or typed above the signature blocks.

REPORT DOCUMENTATION PAGE

Form Approved
OMB No. 0704-0188

1. REPORT DATE *(DD-MM-YY)*	2. REPORT TYPE	3. DATES COVERED *(From - To)*
September 2014	Final	09 July 2013 – 25 April 2014

4. TITLE AND SUBTITLE
METASTABLE PACKAGING FOR TRANSIENT ELECTRONICS

5a. CONTRACT NUMBER
FA8650-13-C-7347

5b. GRANT NUMBER

5c. PROGRAM ELEMENT NUMBER
61101E

6. AUTHOR(S)
Jeffrey S. Moore, Scott R. White, Nancy R. Sottos, John A. Rogers, Bora Inci, Joshua A. Kaitz, Seung-Kyun Kang, Olivia P. Lee, Hector Lopez Hernandez, and Chan Woo Park

5d. PROJECT NUMBER
1000

5e. TASK NUMBER
N/A

5f. WORK UNIT NUMBER
Y0ZA

7. PERFORMING ORGANIZATION NAME(S) AND ADDRESS(ES)
University of Illinois
506 S. Write Street
364 Henry Administration Building
Urbana, IL 61801-3620

8. PERFORMING ORGANIZATION REPORT NUMBER

9. SPONSORING/MONITORING AGENCY NAME(S) AND ADDRESS(ES)
Air Force Research Laboratory
Sensors Directorate
Wright-Patterson Air Force Base, OH 45433-7320
Air Force Materiel Command
United States Air Force

10. SPONSORING/MONITORING AGENCY ACRONYM(S)
AFRL/RYDD

11. SPONSORING/MONITORING AGENCY REPORT NUMBER(S)
AFRL-RY-WP-TR-2014-0152

12. DISTRIBUTION/AVAILABILITY STATEMENT
Approved for public release; distribution unlimited.

13. SUPPLEMENTARY NOTES
This report is the result of contracted fundamental research deemed exempt from public affairs security and policy review in accordance with SAF/AQR memorandum dated 10 Dec 08 and AFRL/CA policy clarification memorandum dated 16 Jan 09. Report contains color.

14. ABSTRACT

Metastable polymeric materials were synthesized, formulated with additives and microcapsules, and then processed into films that served as substrates on which electronic devices were fabricated. New to this effort was the intentional development of depackaging cascades -- the rational design of materials that depolymerize on exposure to specific stimuli. In particular, we investigated acid-sensitive, depolymerizable poly(phthalaldehyde) (PPA), and thermally- and base-sensitive poly(olefin sulfone) (POS) polymers. Conditions for film preparation and fabrication of transient electronics on robust PPA and POS films were optimized. Three degradation triggers -- direct activation by photoacid generation, thermal activation, and mechanical rupture of acid-filled microcapsules -- were investigated.

15. SUBJECT TERMS
transient electronics, triggered depolymerization, low ceiling temperature polymers, degradable polymer films, photo-triggering, thermal activation

16. SECURITY CLASSIFICATION OF:			17. LIMITATION OF ABSTRACT:	18. NUMBER OF PAGES	19a. NAME OF RESPONSIBLE PERSON (Monitor)
a. REPORT	b. ABSTRACT	c. THIS PAGE			Carrie M. Bartsch
Unclassified	Unclassified	Unclassified	SAR	36	19b. TELEPHONE NUMBER *(Include Area Code)* N/A

Table of Contents

Section **Page**

List of Figures

Figure **Page**

List of Tables

Table **Page**

1 SUMMARY

Metastable polymeric materials were synthesized, formulated with additives and microcapsules, then processed into films that served as substrates on which devices were fabricated. New to this effort was the intentional development of depackaging cascades – the rational design of materials that depolymerize on exposure to specific stimuli, resulting in traceless, volatile byproducts.

A complete set of packaging materials was delivered that meets the following criteria: (1) serves as a substrate for device fabrication, (2) encapsulates sensitive electronics to provide temporary protection, (3) undergoes complete disintegration within the specified time of 1 hour, upon triggering by a specific stimulus, and (4) disintegrates without being soaked in water.

2 INTRODUCTION

2.1 Background

Recent exciting and ground-breaking concepts from Rogers *et al.* on transient electronic devices allow data collection and transmission in sensitive areas for a desired time, followed by programmed disintegration and self-resorption.[1] Transient sensors, actuators, power supplies, and wireless control systems were fabricated and wrapped with a silk-based, water-soluble packaging material that is designed to dissolve after minutes to months to years of exposure to water. The active part of the electronic device is composed of semiconductor materials, which operate independently of the dissolving packaging. Such transient electronics offer intriguing possibilities in biomedicine for applications ranging from internal monitoring of wound and infection sites to controlled drug delivery. The novel technology is also potentially useful as environmental monitors placed on buildings, roadways or military equipment to detect structural deformation, temperature change, hazardous agents or suspicious activities for surveillance and reconnaissance. However, before this potential can be realized, improvements must be made in the packaging materials.

During the seedling period, we have surveyed entirely new classes of smart packing materials for transient electronic devices and expanded the modes of transience in important ways. First, stimuli-specific triggers, such as ultra-violet (UV) exposure and heat, enable autonomic device destruction. Following a specific triggering event or upon exposure to particular environments, the packaging or substrate materials break down, exposing the sensitive electronics. Second, the packaging polymers transform from robust barriers, rapidly and on-demand, into small molecular substances that render the electronic devices unidentifiable. Where possible, robust materials degrade into volatile substances, allowing for fabrication of essentially traceless devices. Third, water is not required to dissolve the packaging.

2.2 Approach

To develop metastable packaging materials, we focused on the synthesis of the acid-sensitive polymer, cyclic poly(phthalaldehyde) (PPA), and base- and heat- sensitive poly(olefin sulfone)s (POS). PPA and POS display low ceiling temperatures (T_c), above which the monomers are thermodynamically favored, yet they are stable at room temperature due to kinetic stabilization. Three degradation triggers, direct activation by photoacid generation, thermal activation, and mechanical rupture of acid-filled microcapsules, were investigated in parallel. Processing methods were developed to form robust films with both polymer classes, and fabrication techniques to print transient electronics on polymer films were optimized.

2.3 Scope

For photo-triggered degradation of PPA, photoacid generators (PAGs) were incorporated into the film such that the acid generated upon UV exposure will disintegrate the polymer packaging. We successfully deposited silicon transistors, silicon diodes, and magnesium (Mg) resistors onto the PPA/PAG substrates. Using Mg resistors as a model system, two different PAGs were investigated, triphenylsulfonium triflate (TPST) and 2-(4-(4-methoxystyryl)-4,6-bis(trichloromethyl)-1,3,5-triazine (MBTT). It was found that TPST produced an acid that degraded only the polymer film while MBTT disintegrated both the substrate and the Mg/MgO electronic circuits. As one of the current challenges, the UV-activated MBTT does not erode

electronics frabricated from silicon semiconductors albeit the PPA substrates were completely degraded. The transient behavior of PPA was monitored chemically by Fourier transform-infrared (FT-IR) spectroscopy and physically by dynamic mechanical analysis (DMA). Transience times were reduced by film processing conditions and complete disintegration of transient electronic packaging were achieved in under 1 hour.

In parallel, thermal triggers were investigated with POS polymers as well as acid-containing wax capsules that release acid at elevated temperatures to degrade PPA films. Thermal triggering by radio frequency-induced heating was also explored as an alternative approach. For direct thermal activation, poly(vinyl *tert*-butyl carbonate sulfone) (PVBCS) was prepared and shown to rapidly degrade at 85 °C. Upon thermally initiated degradation, freestanding films of PVBCS degrade into volatile small molecules on a hot stage at 90 °C within 30 min, leaving minimal residue (<3 wt.% by thermogravimetric analysis). For capsule activation, acid was successfully encapsulated in silicone wax microcapsules, and freestanding films of PPA with embedded capsules were fabricated. Thermally triggering the capsules by heating the films at 55 °C released the acidic core contents, thereby degrading the PPA layer.

3 METHODS, ASSUMPTIONS, AND PROCEDURES

3.1 Photo-Triggered Transience of Electronic Devices

3.1.1 Photo-Triggerable Material Development and Characterization

Acid-degradable PPA was synthesized on the gram-scale via cationic polymerization at –78 °C.[2] Molecular weights were determined by size-exclusion chromatography (SEC) using tetrahydrofuran (THF) as the eluting mobile phase. The thermal properties were evaluated by thermogravimetric analysis (TGA) and differential scanning calorimetry (DSC) (Table 1). Nuclear magnetic resonance (NMR) spectroscopy experiments showed that PPA degraded into monomers in chloroform solution upon the addition of deuterium chloride.

Table 1. Synthesis, Molecular weights, and Thermal Properties of Acid-Degradable PPA

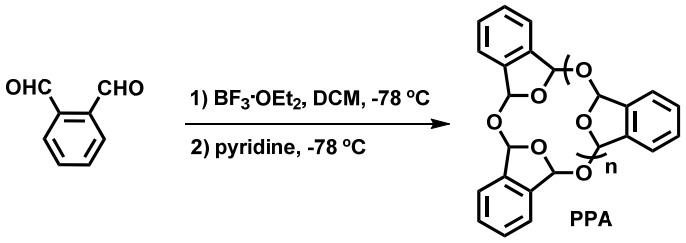

Polymer	M_n	M_w	PDI	T_c	$T_{degradation}$
PPA	154 kDa	403 kDa	2.62	-40 °C	150 °C

3.1.2 Polymer Film Preparation

Films of PPA were prepared by solution drop-cast from 1,4-dioxane with diethylene glycol dibenzoate as plasticizer. Due to the high boiling point and slow evaporation of dioxane, PPA films cast from solution in dioxane (33 mg/mL) exhibit optimal morphology with smooth surfaces and no bubbles compared to other, lower-boiling point solvents. Film thicknesses were tuned by varying solution concentrations; however, at sufficiently high concentrations, the PPA films formed cracks during casting.

3.1.3 Effect of Polymer on Mg Circuit Traces

To demonstrate the effect of polymer on the chemical stability of magnesium (Mg) circuits, we sought to determine if the films of PPA lead to unwanted, spontaneous degradation of Mg traces by resistance measurements. PPA films were drop-cast on top of Mg resistors printed on glass substrates, and we tested for an increase in the resistance over time (Figure 1). The resistor covered with PPA shows a 20-Ohm increase in resistance that plateaued after 5 h, and the resistor remained functional.

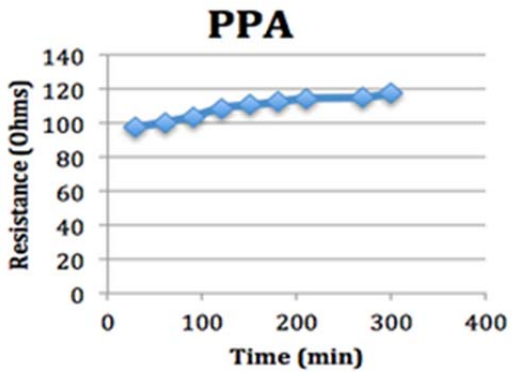

Figure 1. Chemical Stability of Mg Resistors upon Contact with PPA Film

Resistance measurements show that Mg resistors on glass substrates remain functional upon solution drop-cast of PPA films over time.

3.1.4 Printing of Field-Effect Transistors, Diodes and Resistors onto PPA Substrates

To achieve compatibility with transfer printing of the transient circuits, early attempts to fabricate smooth, flat PPA films were performed by "peeling" the polymer film from the glass substrate after solution deposition. Silicon-based active devices were built on the PPA/MBTT films via a combination of transfer-printing technique and electron-beam (e-beam) lithography. Since the polymer substrate is sensitive to UV exposure avoiding it during lithography is crucial. A top silicon-silicon nano-membrane (Si NM, ~200 nm thick) was transfer-printed onto the PPA/MBTT substrate. Next, the gate oxide (MgO, ~80 nm thick) and metal electrodes (Mg, ~300 nm thick) for n-channel metal-oxide silicon field-effect transistors (N-MOSFETs) and silicon p-i-n (PIN) diodes were deposited using e-beam evaporation along with stencil masks. The Mg resistors were deposited via e-beam lithography (Figure 2).

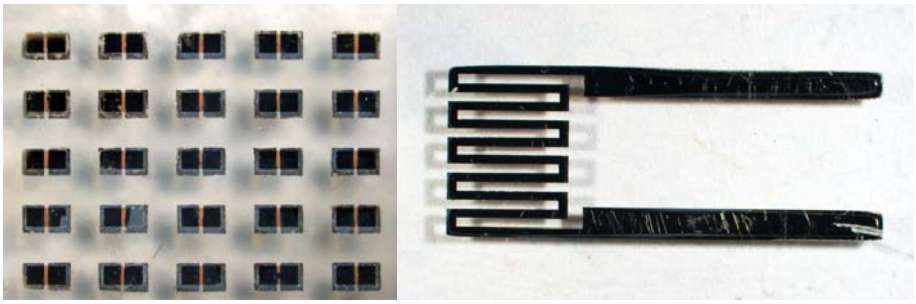

Figure 2. Transient Electronics Deposited on PPA Films

PIN diode array transfer-printed on a PPA film (left), and Mg resistor e-beam evaporated onto a PPA film (right).

3.1.5 Measuring the Transient Resistance of a Mg Resistor on PPA

We were interested in determining the lifetime of the electronics deposited on PPA/photoacid generator (PAG) films. We tested two different PAGs: 2-(4-methoxystyryl)-4,6-bis(trichloromethyl)-1,3,5-triazine (MBTT) with λ_{max} = 379 nm, and triphenylsulfonium triflate

(TPST) with λ_{max} = 233 nm. We tested the change in resistance over time for films exposed to 365 nm and 254 nm source depending on the PAG. The resistance of the films increased when exposed to the UV source, and the films were irradiated until the resistance reached infinity.

Mg resistors were chosen to investigate transient device lifetimes due to the ease of manufacturing and transience testing. E-beam evaporation and stencil masks were used to fabricate the resistors onto PAG loaded PPA films. The free standing films were placed on a glass slide and attached to two Wheatstone bridge probes. Samples were tested with MBTT loadings of 2.5 and 5 mg and three different UV irradiances of 0.20, 0.60 and 1.75 mW cm^{-2}. Figure 3 demonstrates the experimental setup.

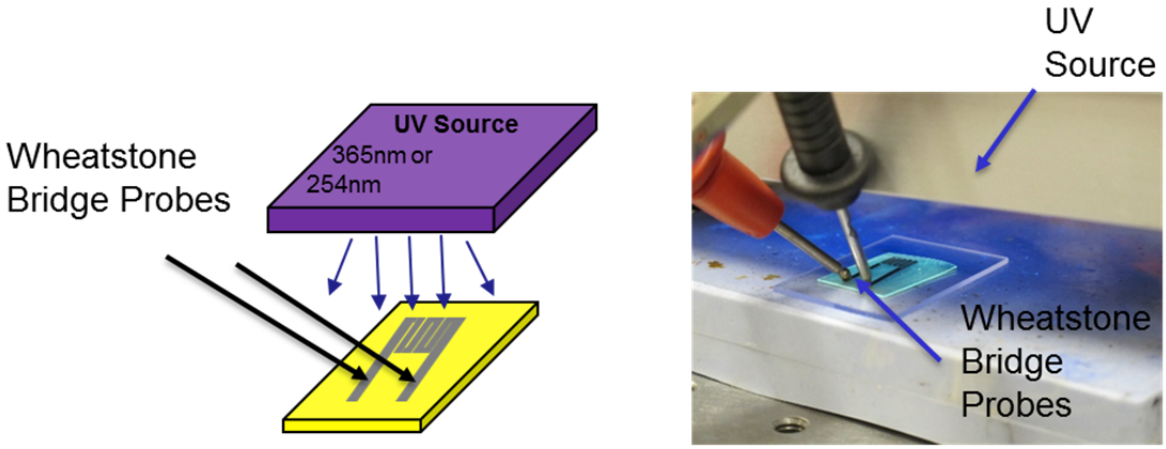

Figure 3. Experimental Set up for Resistance Measurements
Wheatstone Bridge Setup with Mg resistor on PPA/MBTT film

3.1.6 Tracking PAG-Triggered PPA Film Degradation by Infrared (IR) Spectroscopy

In order to verify that PPA degrades into its constituting monomers in the presence of acid, we characterized the blend films and monitored the depolymerization progress by FT-IR spectroscopy. Briefly, a solution of 5 wt.% MBTT/PPA in chloroform was drop-cast onto a sodium chloride plate. Each spectrum was collected after exposing the film to UV (365 nm) light at 30 s intervals, accumulating up to 3 minutes of total UV irradiation time; spectra of the monomer (oPA), MBTT, and PPA were also collected separately for comparison (Figure 4). The spectra of pristine PPA and PPA/PAG blend at 0 s irradiation show a wide band from 900–1150 cm^{-1} for the C-O stretches of acetal but no peak at 1700 cm^{-1} for the C=O aldehyde stretch. As soon as the blend film was exposed to the UV source, the aldehyde peak at 1700 cm^{-1}, matching that of the monomer, appeared and became more pronounced with continued UV irradiation. At the same time, the polymer C-O stretches decreased in intensity. Both of these results suggest the depolymerization of PPA into oPA upon activation of MBTT.

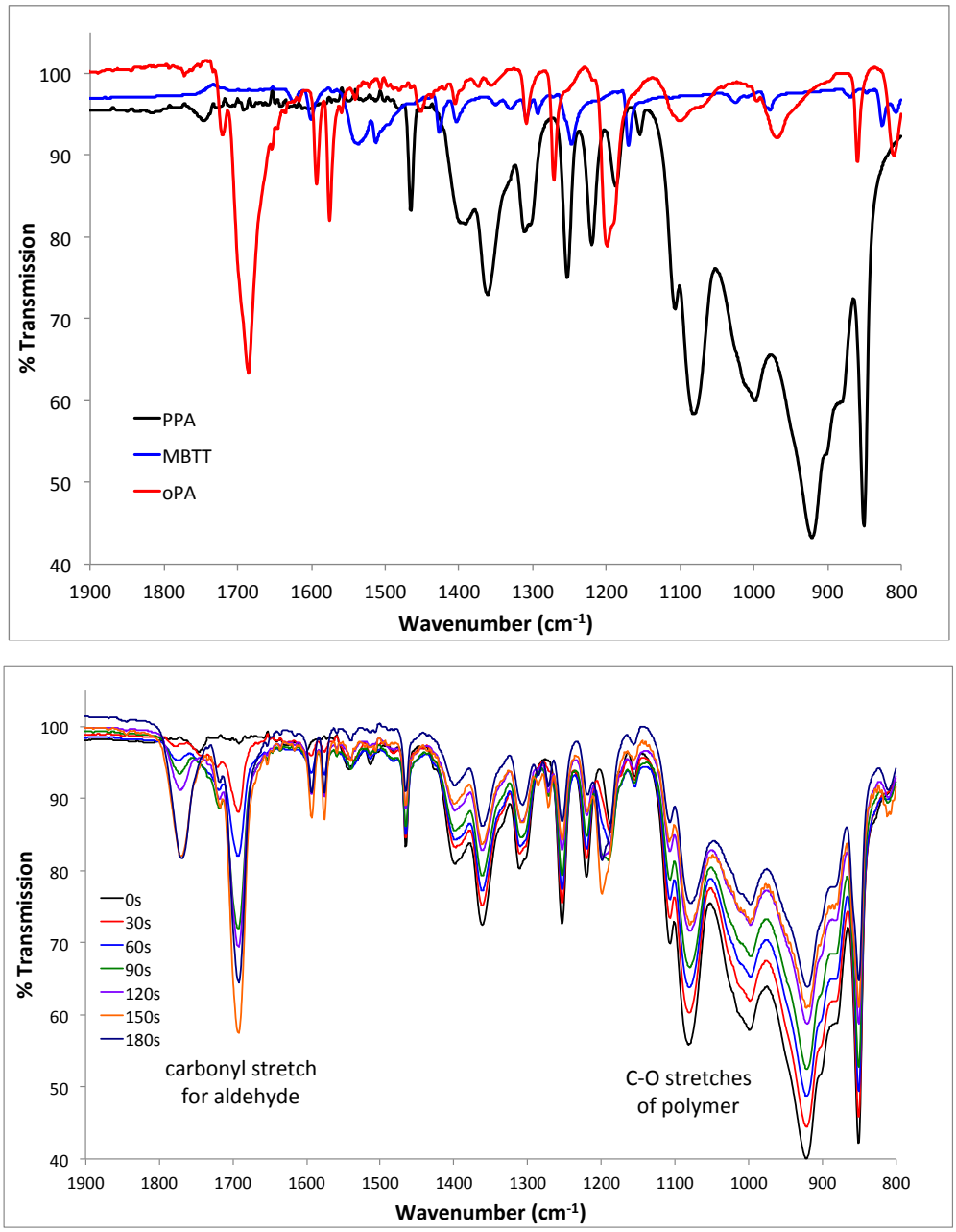

Figure 4. FT-IR Spectra for Chemically Monitoring UV-Triggered PPA Degradation

FT-IR spectra of PPA, MBTT (photoacid generator), and oPA (monomer) (top). The polymer spectrum shows a broad band for C-O stretches from 900–1100 cm^{-1} that is not present in the monomer spectrum, while oPA displays a spectrum with a strong aldehyde peak at 1700 cm^{-1} that is not present in the polymer spectrum. Exposure of the PPA/MBTT blend films to UV light over time leads to the decrease in intensity of polymer C-O stretches and the appearance of monomer aldehyde C=O stretch (bottom).

3.1.7 Mechanical Degradation of PPA Films

We characterized the transience in physical properties of PPA films during UV exposure by monitoring the storage modulus of PPA/MBBT and PPA/TPST while the film is exposed to a UV trigger. As previously mentioned, MBTT is sensitive to light in the long UV range and generates hydrochloric acid while TPST is sensitive to light in the short UV range and generates triflic acid. The acids cleave the PPA backbone and begin the depolymerization of PPA. The samples were tested in time sweep mode on a DMA machine with a static force of 20 g and strain amplitude of 0.075 %. We observed the degradation of the storage modulus for different formulations of PPA films over long UV exposure times to determine the extent of degradation. Two different film formulations were tested with 2.5 and 5 % MBTT/PPA films and two different UV irradiances of 0.7 and 1.75 mW cm^{-2} were used. The samples were tested until the UV exposure causes film tearing and subsequent failure. Current characterization of the light sources is in progress to determine their intensities and exact emission spectrums.

3.2 Thermal and Base-Triggered Transience of Electronic Devices

3.2.1 Base and Heat-Sensitive Material Development and activation

Poly(olefin sulfone)s (POSs) were synthesized by radical copolymerization of an alkyl olefin and condensed sulfur dioxide at –55 °C. The olefins used for the copolymerization are 1-hexene, 2-methyl-1-pentene, and cyclohexene with boiling points at 60–66 °C, 62 °C, and 83 °C, respectively (Figure 5). The resulting polymers—poly(1-hexene sulfone) (PHS), poly(2-methyl-1-pentene sulfone) (PMPS), and poly(cyclohexene sulfone) (PCyHS)—are soluble chloroform and exhibit glass transition, as indicated by TGA and DSC analyses. These properties enable fabrication of POS films by both solution-casting and hot pressing (*vide infra*).

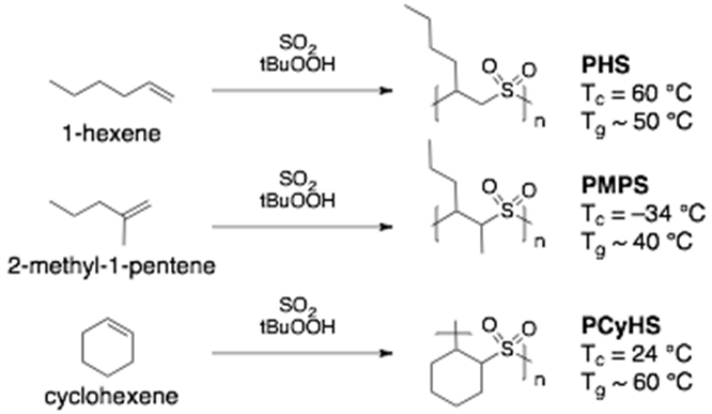

Figure 5. Synthesis of Base-Sensitive Poly(olefin sulfone)s

Preliminary base-triggered degradation of POSs was performed by adding organic bases, including piperidine, 1,8-diazabicycloundec-7-ene (DBU), and P_2-*t*-Bu phosphazene base, into deuterated benzene solutions of PMPS. Characterization of the resulted solutions by proton NMR spectroscopy suggested that P_2-*t*-Bu, a superbase, led to the degradation of the starting polymer in 0.5 h, even though the products were not the expected monomers. In deuterated benzene at room temperature, PMPS did not degrade upon addition of DBU, while the vinyl protons of the olefin monomer began to emerge 0.5 h after the addition of piperidine.

3.2.2 Preparation of POS Films: Solution Drop-Cast and Hot Pressing

Films of POSs were fabricated from both solution and thermal processing. For drop-cast films, PMPS films were deposited from chloroform solution at 70 mg/mL onto Teflon substrates, providing free-standing, transparent films with smooth morphology. POS films were also form by hot pressing the polymer solid at a temperature higher than their glass transitions, the onsets of which were determined by DSC to be 50 °C, 40 °C, and 60 °C for PHS, PMPS, and PCyHS, respectively (Figure 6). To fabricate hot-pressed films, POSs were placed between two Al plates and pressed at 65 °C for 10 min at 140 psi. However, the minimum thickness of hot-pressed films was 350 μm, and the films were less smooth than the solvent-cast ones, extremely brittle, and opaque. We can further improve our methods by increasing the heating temperature much higher than the T_g and allowing longer pressing times so that the polymer has more time to flow.

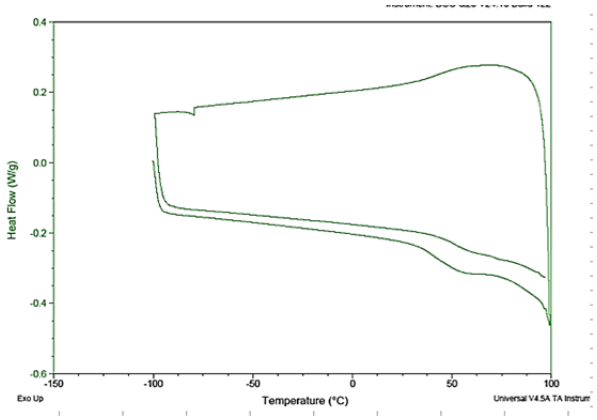

Figure 6. Thermal Characterization of PMPS by Differential Scanning Calorimetry
DSC trace of PMPS shows glass transition with an onset at ~40 °C.

3.2.3 Investigation of Base-Triggered Degradation of POSs

In the literature, it was reported that POSs are prone to base-initiated depolymerization. We conducted preliminary experiments to determine the base-sensitivity of the polymer by submerging the films in piperidine and measured the degradation time. PMPS films of 450 μm degraded in 40 min while films of 60 μm dissolved in 1 min. After showing that the polymer physically degraded, we evaporated Mg electronics by e-beam lithography onto PMPS films and investigated the degradation of the traces and the polymer films (Figure 7). Upon exposure to piperidine, both the circuit and film showed signs of degradation in 10 min and completely disintegrated after 10 h.

Figure 7. Base-Triggered Degradation of PMPS Films
Images show the PMPS film (50 μm) before, during, and at the end of the degradation.

3.2.4 Thermal Activation of POS Films

For direct thermal activation, we used polymers with low degradation temperature, such as poly(vinyl *tert*-butyl carbonate-sulfone) (PVBCS), which degrades at 85 °C (Figure 8). PVCBS was shown to decompose thermally into only volatile products—isobutylene, carbon dioxide, acetaldehyde, and sulfur dioxide, leaving minimal residue.[3] To demonstrate its thermal degradability, we synthesized the polymer and characterized its degradation rate at 4 different temperatures using thermogravimetric analysis (TGA). In these experiments, the furnace is ramped to the desired temperature at 10 °C/min and then held constant for isothermal measurements. Holding the temperature at 70 °C, the polymer degraded to <5 wt% after 1 h while it degraded within 5 min at 90 °C, leaving about 2-3 wt% residues upon complete degradation (Figure 9).

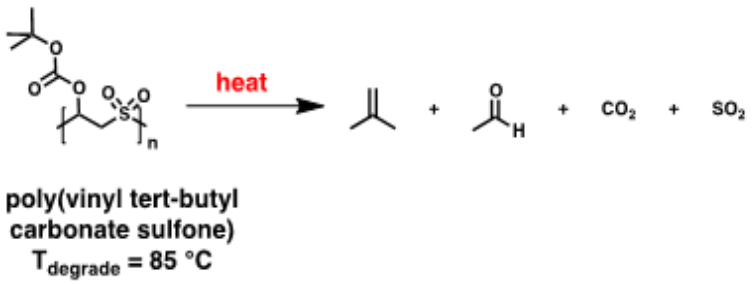

Figure 8. Structures of Thermally Activated Metastable Polymers

To show the feasibility of this thermal degradation under ambient conditions, we processed PVBCS into freestanding films and placed them on a temperature-controlled a hot stage (90 °C). Most of the materials disappeared with minimal residue within 30 minutes (Figure 9). As an immediate target, we aim to investigate ways to reduce the degradation temperature so that the polymer decomposition can be triggered using the RF heater developed by the Rogers group.

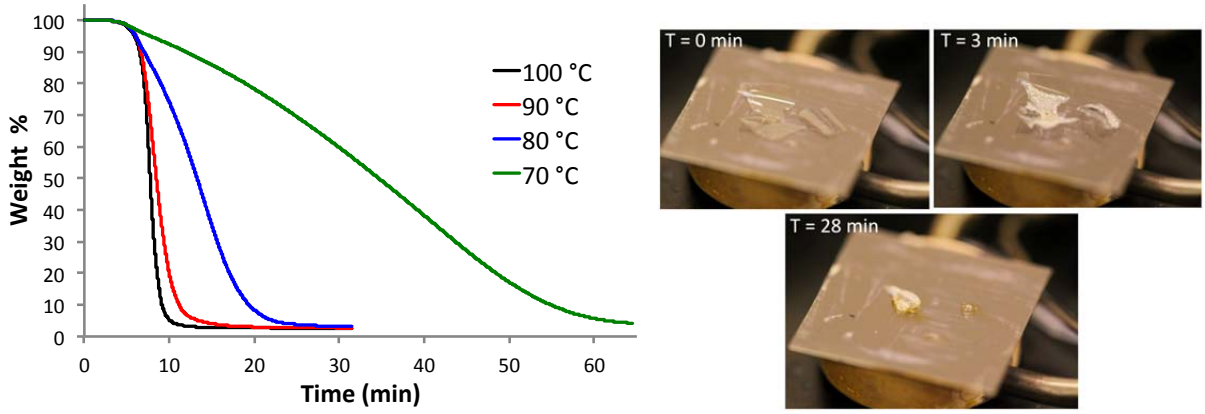

Figure 9. PVBCS Degradation Monitored by TGA and Snap Shots

Isothermal decomposition of PVBCS characterized by TGA (left), and progress of PVBCS film degradation on a hot stage at 90 °C in 28 min (right).

3.2.5 Improving Film Properties of Poly(vinyl *tert*-butyl carbonate sulfone) (PVBCS)

While the degradation properties of poly(vinyl *tert*-butyl carbonate sulfone) (PVBCS) are promising, the polymer molecular weights were relatively low, limiting its ability to form free standing films with sufficient mechanical strength to be used as substrates or packaging. The initial attempt of lowering the catalyst loading from 10 mol% to 5 mol% to 2.5 mol% led to a small increase of molecular weight (M_n) from 11 kDa to 17 kDa to 22 kDa, respectively, as characterized by size-exclusion chromatography (SEC). Increasing the concentration of the reaction mixture by reducing the amount of liquid SO_2 used did not improve polymer molecular weight (M_n = 9 kDa). We hypothesized that the free-radical polymerization may be sensitive to trace impurities. After we rigorously purified the monomer by Kugelrohr distillation and thorough deoxygenation prior to polymerization, we were able to synthesize polymers with molecular weight as high as 108 kDa. This high-molecular weight batch of material still degrade at 85 °C into volatile monomers while forming smooth, free standing films that are less brittle than the earlier batches (Figure 10).

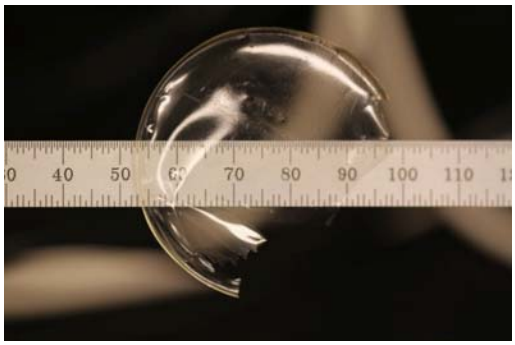

Figure 10. Free Standing Film Fabricated from High-Molecular Weight PVBCS
Films were reliably produced by drop-casting from a chloroform solution.

3.3 Thermal and Mechanical Triggered Transience of Electronic Devices via Embedded Microcapsules

3.3.1 Acid Diffusion into Polyurethane-Poly(urea-formaldehyde) (PU/UF) Microcapsules

Toluene sulfonic acid (TsOH) loaded microcapsules were prepared by diffusing the cargo into microcapsules containing a PU/UF double shell. Following our previously published procedures, we prepared stable PU/UF microcapsules.[3] Briefly, PU prepolymer (Desmodur L 75) was dissolved in the core liquid (ethyl phenyl acetate, EPA), and the solution was emulsified into an aqueous solution of urea, resorcinol and ammonium chloride at a specific stirring rate. After polymerization of PU, an aqueous solution of formaldehyde was added and then allowed a polymerization reaction of UF at 55 °C. Microcapsules with diameter less than 15 μm were prepared by a homogenization method.

These as-prepared microcapsules were immersed in TsOH/ethyl phenyl acetate (EPA) solution at 0.2 M or 0.5 M, and the acid solution was allowed to diffuse into hollow particles at 50°C or

room temperature for desired time. The final TsOH-containing PU/UF capsules were obtained after extensive rinsing and drying. The acidic contents of the PU/UF microcapsules were verified by proton NMR spectroscopy (Varian Unity INOVA, 400 MHz) of core extract. Microcapsule morphology was investigated by scanning electron microscopy (SEM, Philips XL30 ESEM-FEG). TGA was performed on a Mettler-Toledo TGA851 for stability analysis of microcapsule.

3.3.2 Formation of Thermally Responsive Wax Capsules

Our strategy focuses on encapsulating strong organic acids, including benzene sulfonic acid (BSA) and methane sulfonic acid (MSA), in low-melting organic materials, such as silicone wax (m.p. = 43 °C, GPC silicones) and paraffin wax (m.p. = 58-62 °C, Sigma). Superacid-encapsulated wax capsules were prepared by a melt-quench method. Briefly, 3 or 6 mL of MSA or molten BSA at 60 °C was emulsified into 10 g of molten wax at 60 °C containing Span 85 emulsifier to form a primary acid-in-wax emulsion. The primary emulsion was then poured into warm polyethylene-maleic anhydride aqueous solution at 55 °C. After 2 min, the cold water was quickly added to quench microcapsule structure. The microcapsules were collected and dried by vacuum filtration. The acidic contents of the wax microcapsules were verified by TGA analysis (Mettler-Toledo TGA851).

3.3.3 Formation of PEG-Wax Capsule/PPA Double-Layer Film

A film of PPA is first prepared by solvent casting of the PPA solution in chloroform (33 mg/mL) on a polytetrafluoroethylene (PTFE) lined petri dish. By adding pH indicator in the PPA layer, premature release of acid during the process was monitored via observing color change. The wax capsules containing acid were dispersed in an aqueous solution of poly(ethylene glycol) (PEG), poly(ethylene oxide) (PEO) or poly(vinyl alcohol) (PVA), and the dispersion in liquid was deposited on top of the PPA film. The double layer film was air-dried. Thermally induced degradation of the double-layer films was observed using an optical microscope (Leica DMR) equipped with a hot stage for temperature control.

3.3.4 Thermal Activation of Acid-Dispersed Wax Coating

First, a layer of molten silicone (m.p. = 43 °C, GPC silicones) wax was deposited on a film of PPA/pH indicator or glass substrate with Mg resistor by a casting knife film applicator (doctor blade) to protect the PPA portion and Mg traces from acidic dispersion. For thinner protection layers, the molten silicone wax at 70 °C was spin-coated at 2000 rpm for 30 sec while the wax surface was heated by hot air (60 °C). An emulsion of acid-in-wax was prepared by slow addition of acids into molten wax with vigorous stirring at 60 °C, and acidic contents in the emulsion were varied from 20 to 40 wt%. The emulsion was subsequently deposited on top of a wax protected resistor on a PPA film or glass substrate to make a wax layer containing acidic dispersions by doctor-blading, and the applied thickness of the layer was 100 or 200 μm. The thicknesses of these coatings were measured by profilometer (Sloan Dektak 3). The samples were placed on the hot stage for accurate temperature control and resistance changes were measured by the Wheatstone quarter-bridge method during the heating of the samples. Raman analysis was performed on a Raman conformal imaging system (Horiba LabRAM HR 3D).

4 RESULTS AND DISCUSSION

4.1 Photo-Triggered Transience of PPA and Transient Electronics

4.1.1 Solution-Casting of PPA

Solution casting was an effective means for developing high quality films that could be handled, used for lithography, and mechanically tested. Solution casting provided the capability of tuning the desired amounts of PAG, plasticizer, and polymer concentration in solution. This allows for easy modification of the system for testing various film formulations. The optimum solution ratios for PAG loaded films were found to be 2.5-5 mg MBTT : 100 mg PPA : 2.5 mg DGD : 3 mL dioxane. Figure 9 shows one of these films.

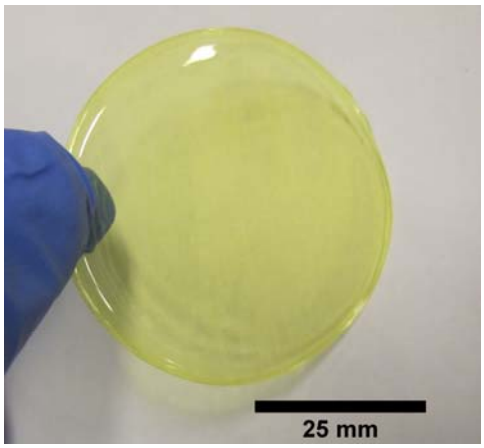

Figure 11. PPA/MBTT Free Standing Film

The films produced from solution-casting can be handled easily and used for lithography and mechanical testing. The mechanical degradation of PPA/MBTT free standing film is characterized by dynamic mechanical analysis (DMA), and the corresponding results can be found in Figure 16 (vide infra).

4.1.2 Electrical Characteristics of Diode and Transistor Arrays

As fabricated, each N-MOSFET displays 30×600 μm channel length and width on PPA/MBTT substrates, and the electrical measurements of these devices show typical on/off ratios $>10^5$ with saturation and linear regime mobilities near 530 $cm^2 V^{-1} s^{-1}$ (Figure 12a). Each PIN diode in an array on PPA/MBTT films consists of a 500×500 μm p-doped region, a 500×500 μm n-doped region, and a 30×500 μm i-region (Figure 12b). The I-V curves show well-defined diode characteristics where the current is almost negligible under 0.12 V but begins to increase sharply after 0.49 V.

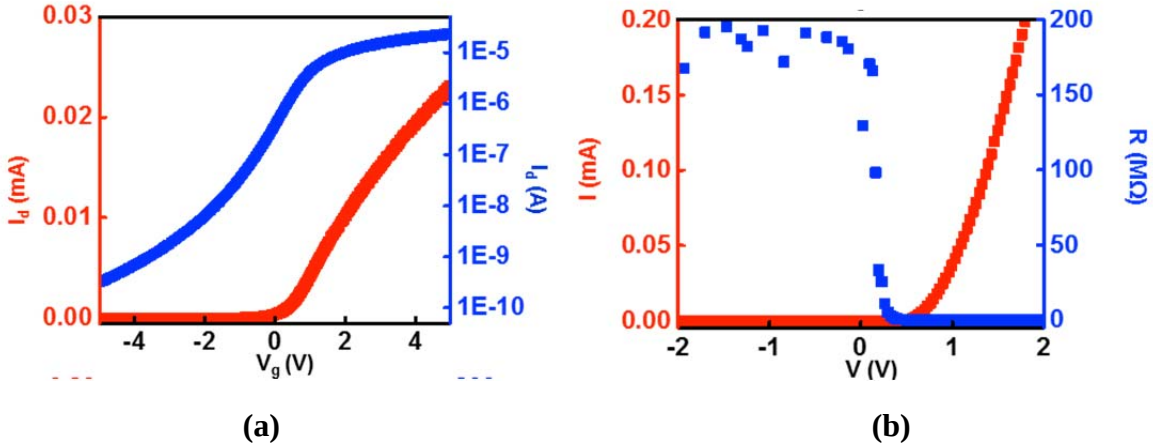

(a) **(b)**

Figure 12. Electrical Characteristics of a N-MOSFET and a PIN Diode Fabricated on PPA
(a) Transfer curve of a transistor on PPA shows that the mobility (linear regime) and on/off ratio are ~350 cm^2 $V^{-1}{\cdot}s^{-1}$ and ~10^5, respectively. (b) The I-V curve of the diode shows defined diode characteristics

4.1.3 Electrical Transience of Mg Resistors

All samples tested exhibit an initial increase in resistance that continues at an increasing rate until sample failure. We found that controlling the loading of MBTT provided control for the rate at which the degradation of the resistor occurred. The generation of HCl from MBTT and the degradation of PPA both contributed to the degradation of the resistor. To determine the individual role of MBTT on the initial increase in resistance, a Mg resistor on a 5 % MBTT/polystyrene film was fabricated and tested. The resistance initially increased at the same rate as the 5 % cPPA/MBTT sample but then quickly plateaued (Figure 13). The plateau observed in the 5 % polystyrene/MBTT sample was not observed in the 5 % PPA/MBTT sample. This result indicates that the PPA and MBTT are both needed for rapid degradation times. It is possible that the acid is more mobile in the cPPA and begins to flow when PPA begins depolymerizing, as opposed to the polystyrene film that is unaffected by acid generation.

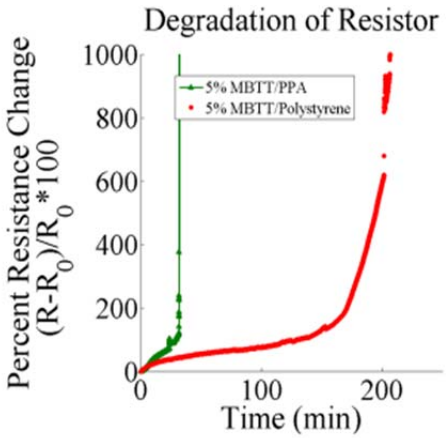

Figure 13. Comparison of the Degradation Behavior between PPA and Polystyrene Films
The resistance of 5 % MBTT in PPA/polystyrene film initially increased at the same rate as the 5 % MBTT in PPA/MBTT sample but then quickly plateaued.

In PPA/MBTT films we observed that at 1.7 mW cm^{-2}, the MBTT concentration had little effect on the resistance. Shown in Figure 14, both the 2.5 and 5 wt% sample resistances increased at the same rate and reached a 100 % change in resistance within 20 minutes. At this irradiance, both samples apparently generate sufficient HCl to achieve a maximum degradation rate of the resistance for a Mg resistor. However, at the lower irradiances of 0.60 and 0.20 mW cm^{-2} the resistance of the 2.5 % films exhibit a much slower rate of degradation. At these irradiances plateaus can be seen in the 2.5 % cases that do not occur in the 5 wt % samples. The 2.5 % samples reach a 100 % change in resistance within 90 and 110 min for irradiances of 0.60 and 0.20 mW cm^{-2} respectively, while 5 % samples reach a 100% change in resistance within 35 and 70 min.

After enough time and exposure to UV, the PPA substrate degrades and deforms, causing the resistor to completely fail. This deformation can be observed in the transient resistance data in the 2.5 wt% case where the resistance data becomes very noisy right before failure. The deformation of the PPA for the 5 mg MBTT case occurs but cannot be seen in the resistance data because of the extensive degradation caused by the interaction between HCl and Mg up to 800 %, which masks the fluctuations induced by the deformation of the film. Importantly, once the resistors have failed, the UV-source was removed and the remaining film and Mg traces continued to erode in the presence of the generated acid. The accompanying images show films before testing, immediately after failure, and 72 h later. It can be seen that the Mg traces do not physically disappear after the electronic functionality has been destroyed, but after 72 h the sample is almost entirely unrecognizable.

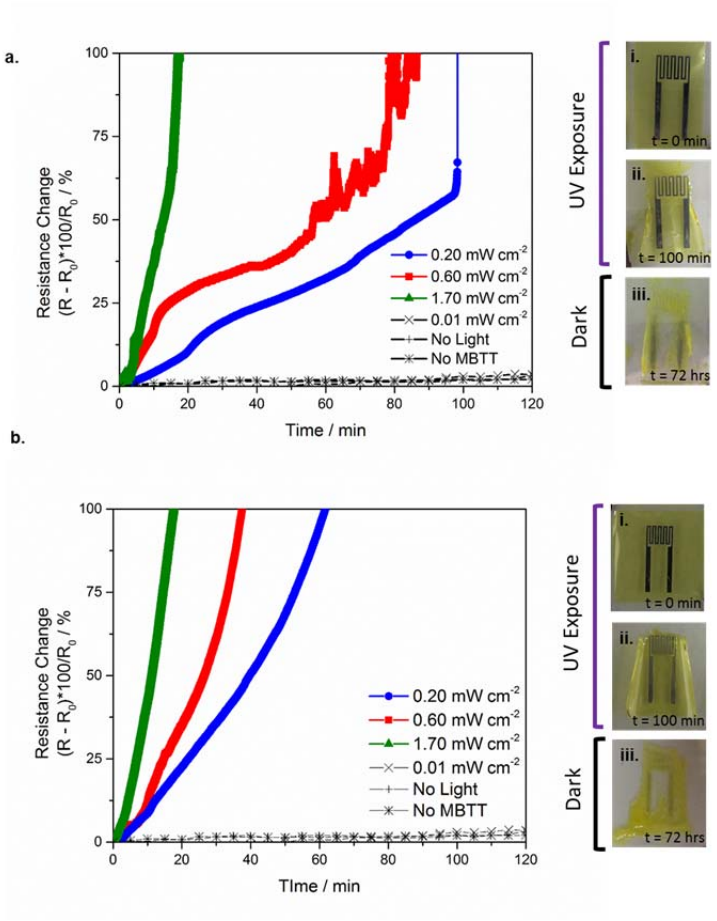

Figure 14. Electrical Transience of Mg Resistors on PPA/MBTT Films

Resistances of (a) PPA films containing 2.5 % of MBTT and (b) PPA films containing 5 % MBTT increased at the same rate and reached a 100 % change in resistance within 20 min.

Interestingly the use of TPST, which generates triflic acid led to a different degradation behavior where the polymer was degraded but the Mg traces were largely unaffected on the time scale of the test. This contrast in behavior between MBTT and TPST is shown in Figure 15. This might prove as a useful selective targeting system in future systems development.

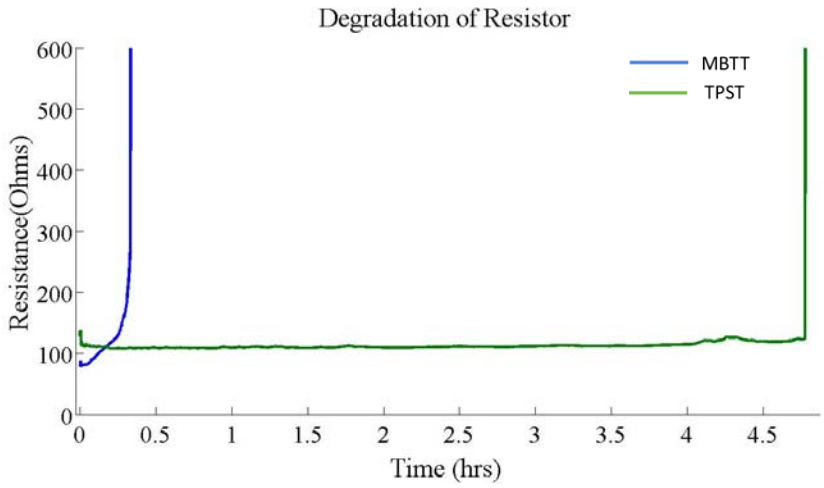

Figure 15. Degradation of Resistors

The blue curve represents a film containing MBTT while the green curve represents a film containing TPST. Films are similar thickness 35-40µm.

4.1.4 Mechanical Transience

We found that MBTT works much more quickly at degrading the PPA and exhibits an exponential decay in storage modulus while the TPST creates a rapid initial decrease in modulus but then a slow long linear degradation of the PPA. The reasoning for this is still under investigation. Similar to the electronic lifetime of the transient resistor samples, the mechanical degradation of PPA can be controlled by controlling the intensity of the UV source. Figure 16 demonstrates the average degradation behavior of the films that were tested.

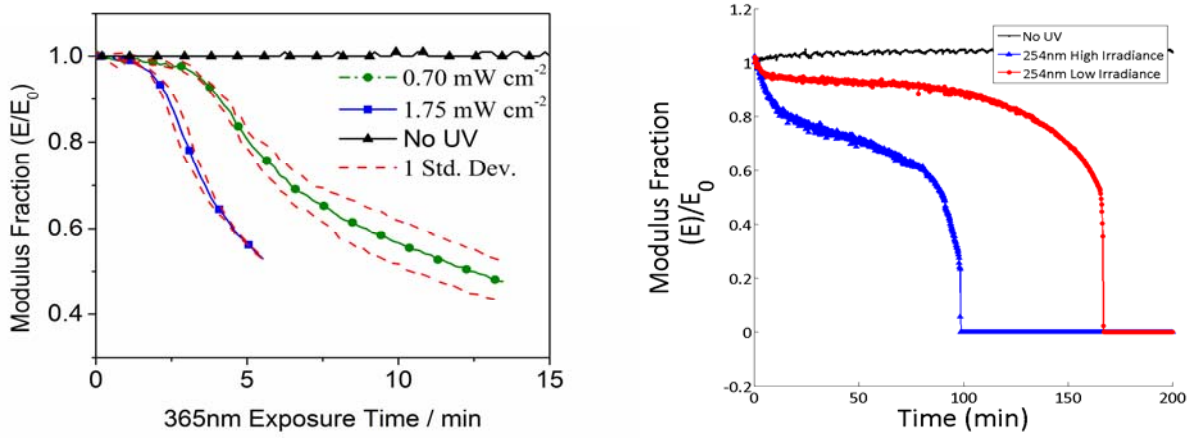

Figure 16. Mechanical Degradation of PPA Films with Different Photoacid Generators

PPA films loaded with 2.5 % MBTT and TPST were continuously exposed to designated UV source for the duration of the test until failure. Time sweeps results show that MBTT is more efficient at degrading the PPA films than TPST.

We observed significant decreases in the storage modulus of 2.5 % MBTT/PPA films of up to 66 % before film tearing. Film degradation for all conditions tested occurred in two different stages. There is an initial lag time where the modulus barely decreases during exposure to UV light, but then a second stage initiates a drastic and rapid decrease in modulus. We believe this is due to the time needed to generate acid and sufficiently degrade PPA to affect its storage modulus. Once enough time passes, the PPA begins to lose much of its storage modulus very quickly. The 2.5 % MBTT/PPA samples took an average of 7 min to reach failure when exposed to 1.70 mW cm^{-2} and 15 minutes when exposed to 0.70 mW cm^{-2}. Once a sample has failed, it loses all load carrying capability and has lost much of its solid like properties.

4.2 Activation of Transience via Embedded Microcapsule Rupture

4.2.1 Acid Diffusion into PU/UF Microcapsules

We developed a new technique to incorporate organic superacids by diffusing the cargo into microcapsules containing a PU/UF double shell and EPA core. The PU/UF EPA capsules were prepared by emulsification polymerization reaction, and the capsules with diameter of 75-250, 45-75, and 20-45 μm were separated by sieving.[4] Microcapsules with diameter less than 15 μm were obtained by homogenization of emulsion before the polymerization reaction.

Acid-filled microcapsules were successfully prepared by diffusing a solution of *p*-toluenesulfonic acid (TsOH) in EPA into the as-prepared capsules (75-250 μm). To determine the amount of time needed to perform the acid diffusion, the acid concentration of TsOH/ethyl phenyl acetate (EPA) solution in the capsule core was quantitatively measured and analyzed by proton NMR spectroscopy. We found that the TsOH concentration increased with immersing time, and the average concentration values were 37 mM, 53 mM and 60 mM after 6 hours, 1 day and 2 days of immersion, respectively (Figure 17a). We also examined the effect of agitation on the acid diffusion. The empty capsules were immersed in acid solution at 0.5 M and stirred for 1 day with spiral propeller type mixer blade (40 rpm). The TsOH concentration in the agitated capsules was 52 mM, which is similar to that of non-agitated capsules (53 mM), indicating that agitation shows minimal effects on the extent of acid diffusion. While particles with sizes in the range of 75–250 microns contain the highest amount of acid, the acid diffusion into the smaller PU/UF EPA capsules was less effective. The average acid concentration values in core of 45-75 μm, 20-45 μm and 5-15 μm sized capsules were 9.3 ± 3.4 mM, 11.3 ± 4.7 mM and 13.9 ± 2.2 mM, respectively, after 1 day of immersion.

The stability of the PU/UF capsule containing TsOH/EPA was determined by thermal gravimetric analysis (TGA). All capsules showed similar TGA traces regardless of immersion time, and the capsules were stable up to ~200 °C (Figure 17b). To verify whether acid diffusion lead to the damage of a capsule shell, the morphology of capsules was observed by scanning electron microscopy (SEM). Images obtained via SEM showed no significant alterations of the capsule shell even after 2 days of immersing in TsOH/EPA. (Figure 17c).

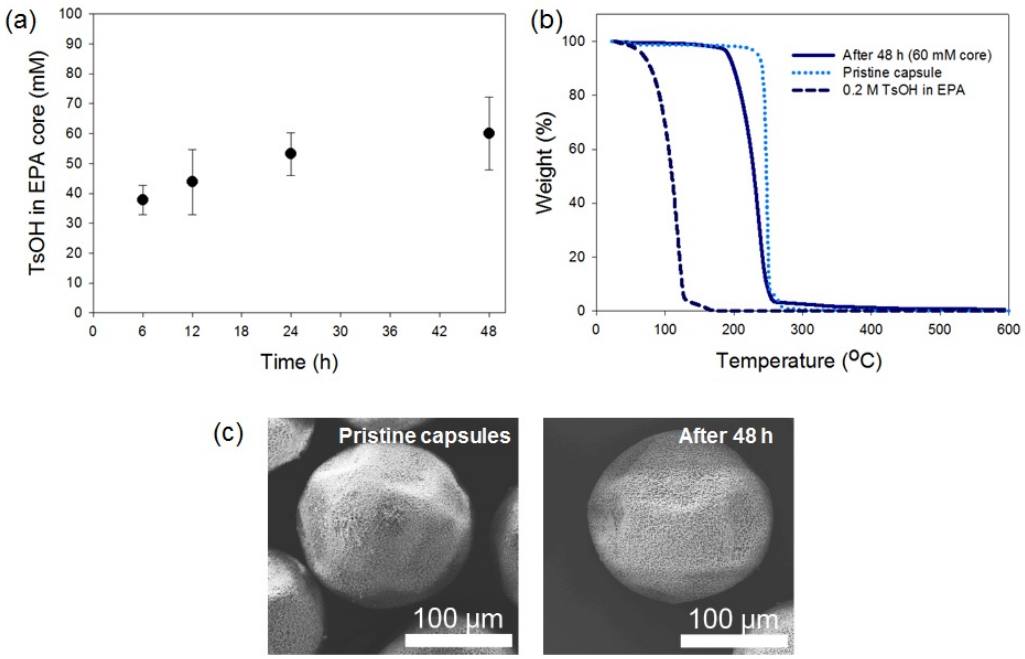

Figure 17. Stability and Morphology of Microcapsules Filled with *p*-Toluenesulfonic acid
(a) TsOH concentrations within the capsule core rises with increased diffusion time. (b) TGA traces of the PU/UF capsule containing TsOH/EPA after 48 h of immersion. (c) SEM images of pristine PU/UF EPA microcapsules and TsOH-filled microcapsules by diffusion.

Before incorporating acid capsules into polymer films, we examined acid-triggered film degradation by crushing the TsOH-containing PU/UF capsules on top of PPA films. Crushing the capsules between glass slides released a large amount of the acidic core solution, and the film was degraded. Upon drying the films in a vacuum oven over 24 h, we observed the formation of a yellow residue (Figure 18). A control experiment was performed with EPA-containing PU/UF capsule, and the treated PPA film showed dissolution of PPA and subsequent solvent evaporation.

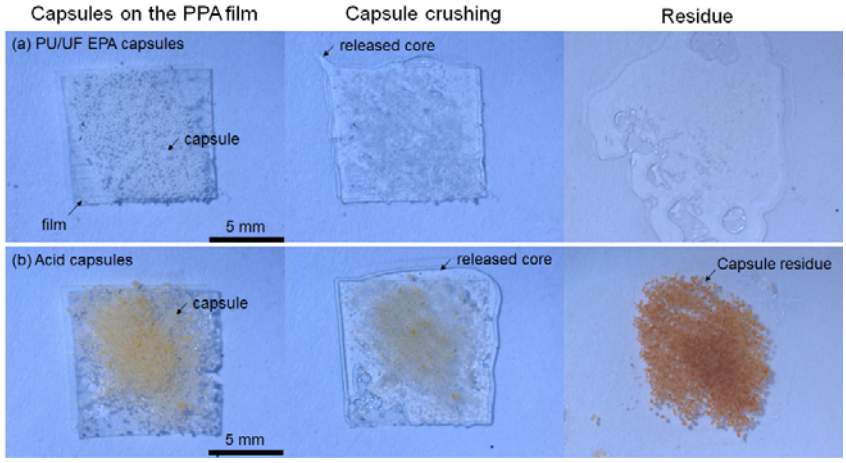

Figure 18. Degradation of PPA Films by Rupture of Acid-Filled Microcapsules
Changes of PPA films after (a) EPA (control) and (b) acid capsule rupture.

Proton NMR spectroscopy was performed to analyze the degradation of PPA films treated with acidic core solution. A 50-μm PPA film (5 mg) was treated with 10 μL of TsOH in EPA (37 mM), and the degradation was allowed to proceed for 1 day. Prior to the NMR analysis, the residue was dissolved in $CDCl_3$, and its NMR spectrum showed characteristic peaks of *o*-phthalaldehyde (*o*PA) as the degradation product along with the disappearance of the PPA peaks (Figure 19a). This result demonstrates that the acidic capsule core is effective for degrading PPA.

We also measured the weight loss of PPA films (2.11 mg) after applying the TsOH/EPA solution (37 mM, 6.39 mg) by TGA analysis under nitrogen atmosphere at 25 °C (Figure 19b). Although this result does not represent the weight loss of PPA over time because EPA in the sample evaporates, the final weight of residue (1.03 mg) after 38 h is less than initial film weight. As the next step, we will further investigate the cause and mechanism of PPA weight loss.

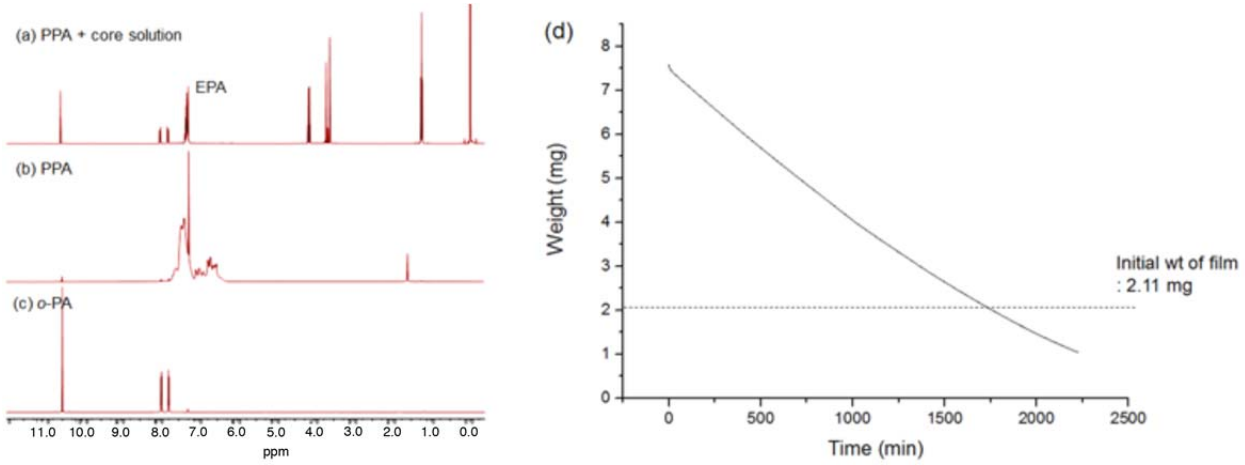

Figure 19. Characterization of PPA Degradation Triggered by Acid Microcapsules

NMR spectra of (a) PPA film treated with the acid core solution, (b) PPA film, and (c) o-PA, monomer of PPA. (d) An isothermal TGA trace of PPA film treated with the acid core solution at 25 °C after 38 h.

Degradation experiments were performed with free-standing PPA and poly(*o*-(α-methyl)benzaldehyde (PMBA) films embedded with TsOH-filled capsules. The capsules were incorporated by solution-casting onto Teflon substrates, even though they did not appear to be fully immersed in the film. Base on the SEM analysis, the PPA polymer near the capsules appears degraded, likely due to the residual acid on the particle surface. The use of smaller particle sizes does not affect the morphology much. For this reason, the stability of the capsule needs to be improved, and we aim to overcome this limitation by developing coatings that will prevent acid leakage and subsequent localized degradation.

We ruptured the capsules by pressing the film between glass slides. The resulting film degradation was observed optically, and the residue was characterized by NMR spectroscopy. Optically, the films containing acid-diffused capsules completely lost their physical properties and structure. PPA fully converted into monomer; while PMBA seemed to be less sensitive to acid trigger based on NMR analysis, the film still lost its physical properties (Figure 20). Control samples embedded with EPA capsules were used to differentiate between the effect of the TsOH/EPA and EPA in the capsules. The control samples showed mostly dissolution and

reformation of the polymer films, where PPA films remained cracked while the PMBA remained a free-standing film.

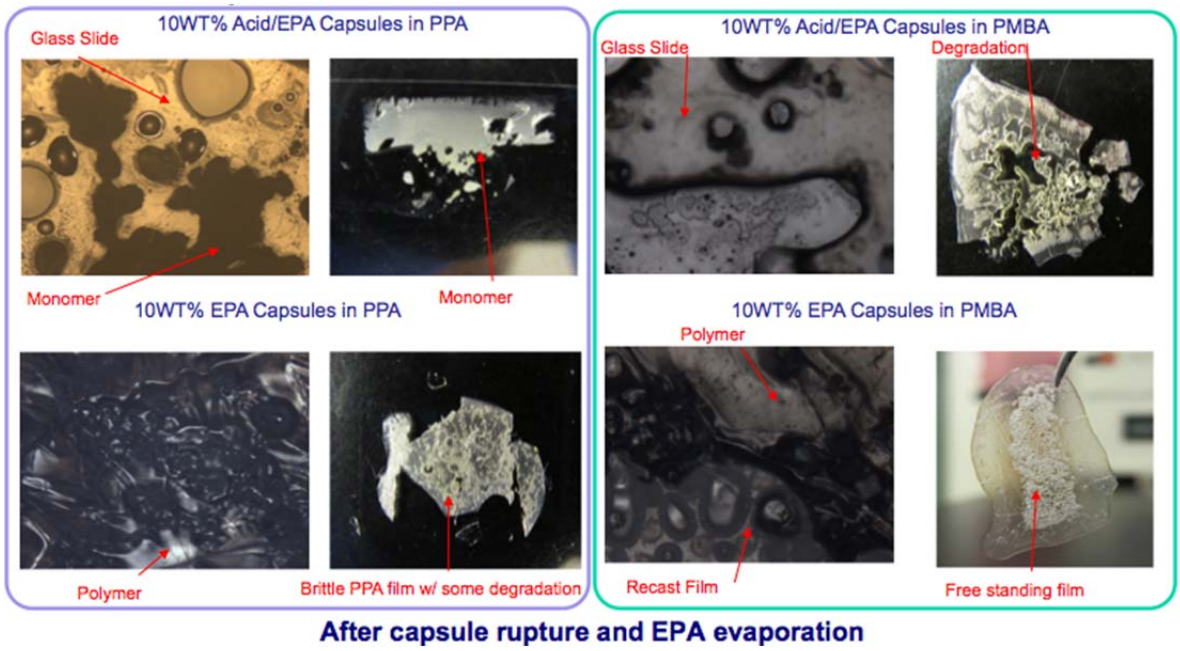

Figure 20. Optical Microscope Images of Acid-Sensitive Polymer Films Triggered by Rupture of Embedded Microcapsules

Degradation of PPA (left) and PMBA (right) films triggered by physically rupturing the embedded acid-containing microcapsules

4.2.2 Activation of Thermally Responsive Wax Capsules

We developed heat sensitive microcapsules with acidic core contents that can degrade acid-sensitive polymers such as PPA and Mg electronics. Our strategy focuses on encapsulating strong organic acids, including benzene sulfonic acid (BSA) and methane sulfonic acid (MSA), in low-melting organic materials, such as silicone wax (m.p. = 43 °C) and paraffin wax (m.p. = 58-62 °C). We hypothesize that localized induction heating of electronic device will trigger the melt transition of wax and the release of the microcapsule cores, triggering depolymerization of the substrate and disintegration of the electronics. With this strategy, the electronic device itself can control the heating and subsequent destruction of the device without external stimuli such as UV irradiation.

Superacid-encapsulated wax capsules were prepared by a melt-quench method. The molten acid was emulsified into molten silicone wax in a warm aqueous solution, and the microcapsule structures were then quenched by the addition of cold water. For the preparation of paraffin wax capsules, the acid-in-wax emulsion was not stable, thereby reducing encapsulation efficiency and acid contents (10 wt%), and the final microcapsules were sticky. On the other hand, silicone wax, which has a much higher molecular weight (12.6 kDa) than paraffin wax, formed a stable emulsion due to high viscosity of the wax in the liquid state. Silicone capsules containing acid cores were obtained, and shells were harder than paraffin wax capsules. SEM analysis showed

that the silicone capsules have multiple acid core structures (Figure 21). The weight percentages of MSA and BSA in capsules were 48 wt% and 21 wt%, respectively based on the TGA.

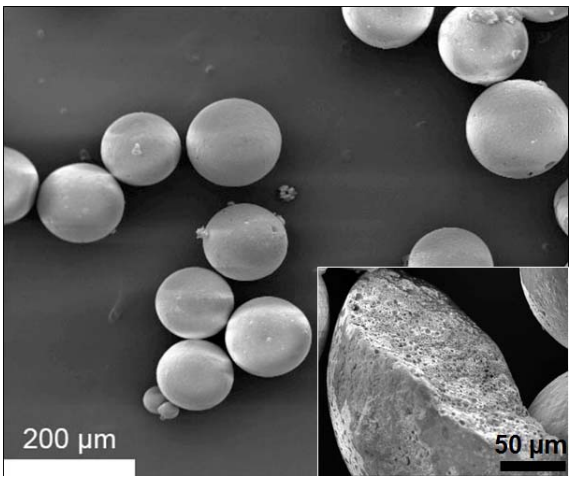

Figure 21. SEM Image of Silicone Wax Microcapsules

Each spherical microcapsule in the micrograph consists of a silicone wax shell wall with a BSA core.

In order to make small (1-20 µm) wax capsules, homogenization or sonication was used when the acid-in-wax emulsion was poured into warm water. Without sonication, the smallest capsules attainable by mechanical stirring were on the order of 75-125 µm. Sonication of the emulsion allowed us to obtain capsules smaller than 20 µm in diameter. However, characterizing the microcapsules using TGA showed that the capsules prepared by sonication do not contain acid in the cores. It is expected that the diffusion rate of acid from wax droplets to water is very high because of the small wax droplet size. Thus, much of the acidic core content was lost during encapsulation.

Prior to incorporating acid capsules into polymer films, we examined thermally triggered film degradation by melting silicone wax/BSA capsules placed on the PPA film. Degradation of PPA films was observed under an optical microscope equipped with a hot stage for temperature control (20 °C/min ramp from room temperature to 55 °C). Since both silicone wax (m.p. = 43ºC) and BSA (m.p. = 51 °C) are solid at room temperature, they can undergo phase transition to liquid at temperature above their melting points and spread out on the film. After 12 s at 55 °C, the PPA film began to disintegrate, and its majority disappeared within 30 s (Figure 22). As the next step, we plan to investigate methods to embed capsules in PPA films.

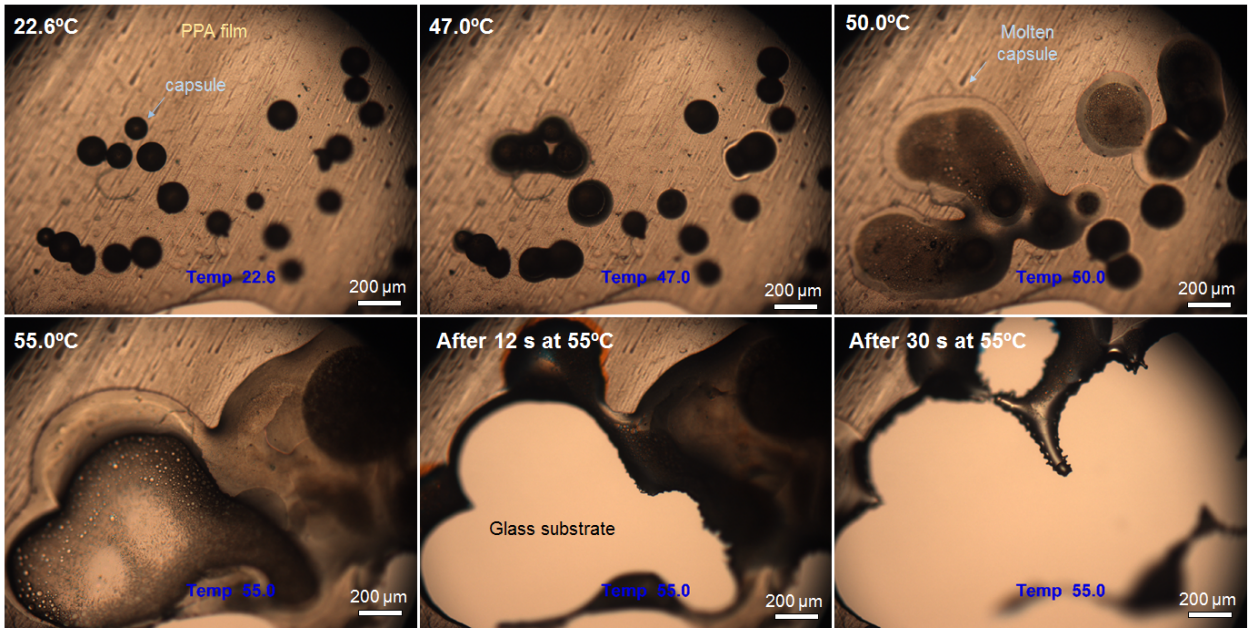

Figure 22. Degradation of PPA/Silicone Wax Films by Thermal Activation

A PPA film with silicone wax/BSA microcapsules on top is thermally triggered to degrade. As the hot stage temperature increases, both the silicone wax and BSA melted to induce PPA depolymerization.

4.2.3 PEG-Wax Capsule/PPA Double Layer Film

While the silicone wax capsules are promising, embedding the capsules in PPA films by solution-casing is challenging because silicone wax and PPA exhibit similar solubility. It was shown that many poor solvents for silicone wax eventually destroyed the microcapsule structure. One way we approached the challenge is to embed the microcapsules in a different polymeric material. In this case, a film of PPA was first prepared, and a suspension of particles in dissolved polyethylene glycol (PEG) or polyethylene oxide (PEO) was then deposited on top of PPA (Figure 23). PEG is chosen as the second polymer layer because the polymer has low melting points (43-65 °C), depending on molecular weight, and good solvents for PEO (water) do not dissolve the silicone wax. We prepared double layer films with PEO (2,000 kDa, m.p. = 63-65 °C) and PEG (1.4 kDa, m.p. = 42-46°C).

Thermally induced degradation of the double-layer films was observed using an optical microscope equipped with a hot stage for temperature control. By adding a pH indicator to the PPA layer, the rupture of the wax microcapsules and subsequent degradation of the films were visualized (Figure 23). The double-layer films consisting of low-melting PEO-wax capsule layer showed a color change of the PPA layer by released acidic contents at 55 °C. In contrast, a control sample consisting of a PVA-capsule layer did not show any color change up to 80 °C, and the molten wax and acid core were contained within the PVA layer without spreading. This result demonstrates that melting the PEO or PEG layer is important to deliver released acidic contents to the PPA layer.

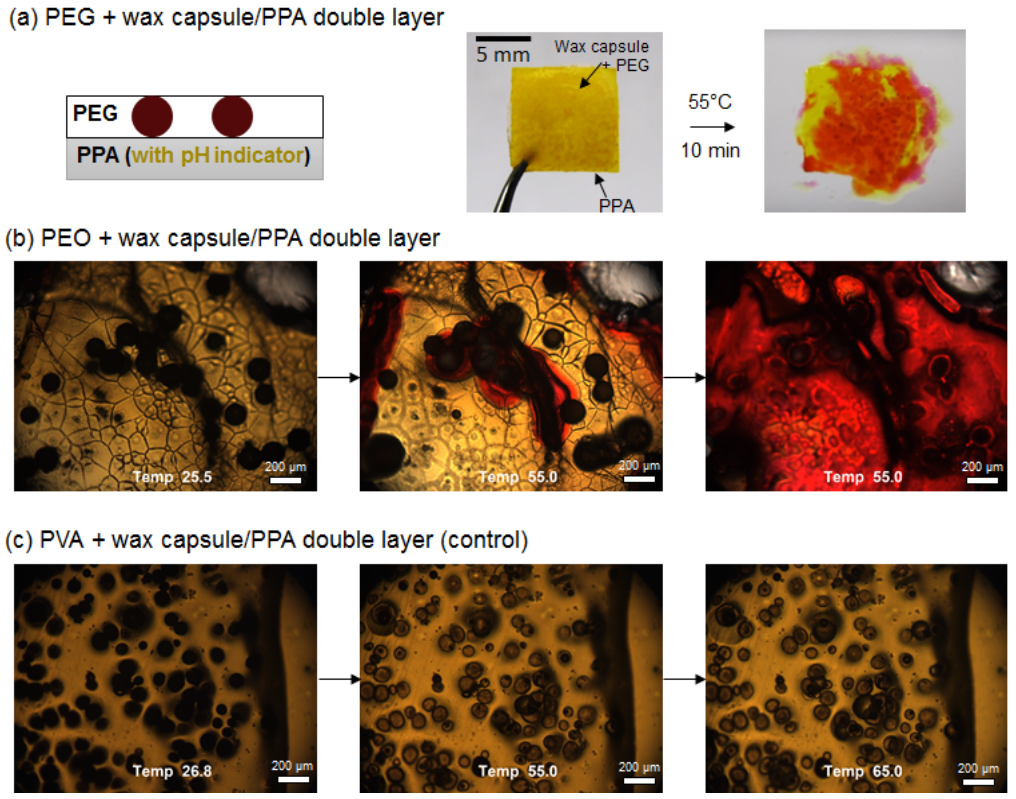

Figure 23. Thermal Triggering of Free-Standing Double Layer Films

The films consist of (a) low-melting PEG layer, (b) low-melting PEG layer and (b) high-melting PVA layer (control) on top of PPA films, and the degradation was thermally activated by heating at 55 °C.

4.2.4 Acid-Dispersed Wax Coated Mg Resistors on Glass

Alongside wax microcapsules for thermal activation, we have developed a heat sensitive wax coating containing solid or liquid acidic dispersion. (Figure 24a) First, a layer of molten silicon wax was deposited on the Mg resistor on glass by spin coating to protect the resistor from acidic dispersion. The thickness analysis of coating by profilometer proved that the protection layer has uniform surface with 14.41 ± 0.88 µm of thickness (Figure 24c). An emulsion of acid-in-wax was subsequently deposited on top of the wax/resistor to make this wax layer-containing acidic dispersions (MSA or BSA). The applied thicknesses of acid/wax coating by doctor-blading were 100 or 200 µm, and actual thicknesses of the coating were found to be 45 and 93 µm, respectively based on the profilometer analysis (Figure 24c). It indicates the coating thickness is well-controllable. Acid dispersions in wax coating were observed by optical microscope, and the dispersions were spherical and smaller than 20 µm regardless of the type of acids (Figure 24b).

The resistance change of the resistor was observed for a month to confirm stability of the acid/wax coating before thermal triggering, and there was no resistance change up to a month. In the absence of a protection layer, however, a direct coating of acid/wax on Mg resistor immediately increased a resistance 45 times higher compared to the pristine resistor.

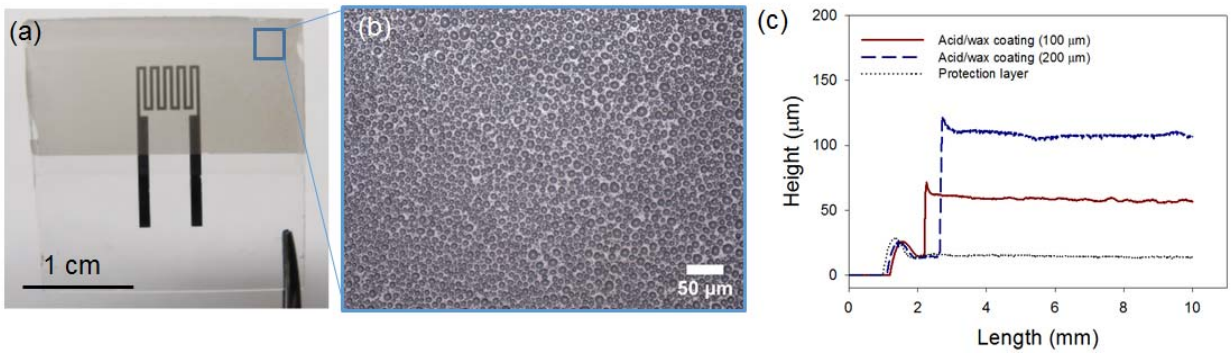

Figure 24. Images and Film Thickness of Acid-Dispersed Wax Coated on Glass

(a) MSA/wax coated Mg resistor on glass, (b) optical microscopy image of MSA dispersions in wax coating, and (c) surface profiles of protection layer, acid/wax coating layers with different coating thicknesses on Mg resistor.

To determine temperature dependent degradation of Mg, we heated the resistors on glass with MSA/wax coating (20 wt%) at 45, 55, and 65 °C. (Figure 25) At 45 °C, the film degraded much more slowly than at 65 °C as the rapidly melting wax coating could induce fast degradation of Mg resistors. To verify the effect of acid amount in wax coating, acidic contents were varied from 20 wt% to 40 wt% while the trigger temperature was maintained at 55 °C. As expected, coatings containing large amount of acids led to fast degradation of the resistor, and failure of the resistor was achieved within 2 min from the 40 wt% acid/wax coating at 55 °C.

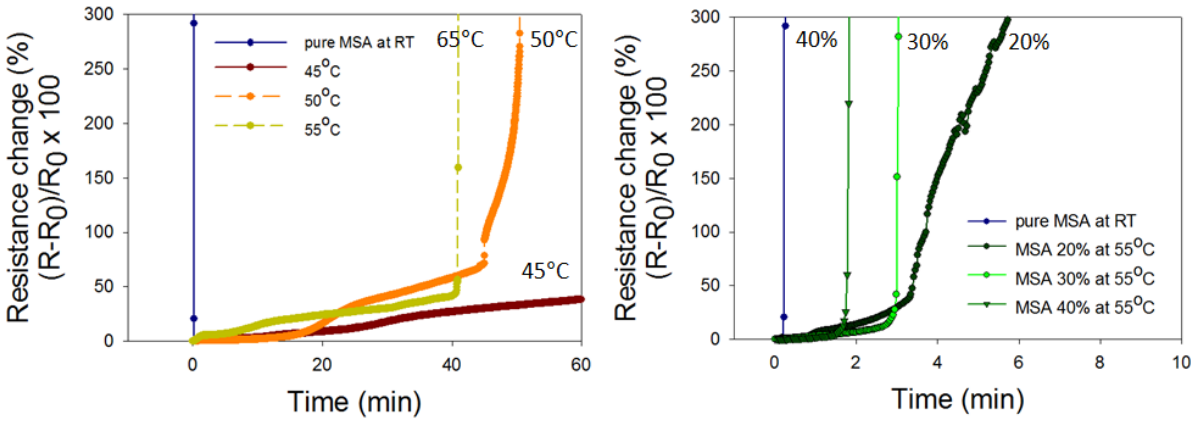

Figure 25. Thermally Triggered Electrical Transience of Resistors on Acid-Disperson/Wax-Coated Glass Slides

Resistance change induced by melting of MSA/wax coating was determined at different temperatures (left) and weight percent of MSA in the coating (right).

4.2.5 Acid-Dispersed Wax Coated Mg Resistors on PPA

Though Mg electronics can be destroyed by released acids, Si-based electronics are not degradable by MSA. For this reason, PPA was employed as a substrate to achieve entire disintegration of electronics by degradation of Mg electronics and PPA substrate. First of all, preparation and thermally-activated disintegration of a Mg resistor on PPA was tested. A Mg resistor was deposited on PPA by electron-beam evaporation with high resolution stencil masks. And, the MSA dispersed wax coating with a protection layer was deposited on a Mg resistor as

described above. As shown in Figure 26a, a free-standing resistor on PPA with acid/wax coating could be prepared.

To show the feasibility of this wax coating for thermal activation, we placed the acid/wax coated resistor on a temperature-controlled a hot stage at 55 °C. (Figure 26b) The melting wax led to degradation of Mg by acid and generated bubbles by following the metal-acid reaction.

$$Mg + 2HA \rightarrow MgA_2 + H_2\,(g) \qquad (1)$$

On the other hand, degradation of the PPA substrate was visualized by generation of brown residues which are believed to be *o*PA monomers. The wax-coated PPA films with acidic dispersions showed disintegration of the PPA layer and resistor within 1 min at 55 °C upon the melting of the wax coating, and this method was shown to be a viable approach for disintegrating electronics on PPA.

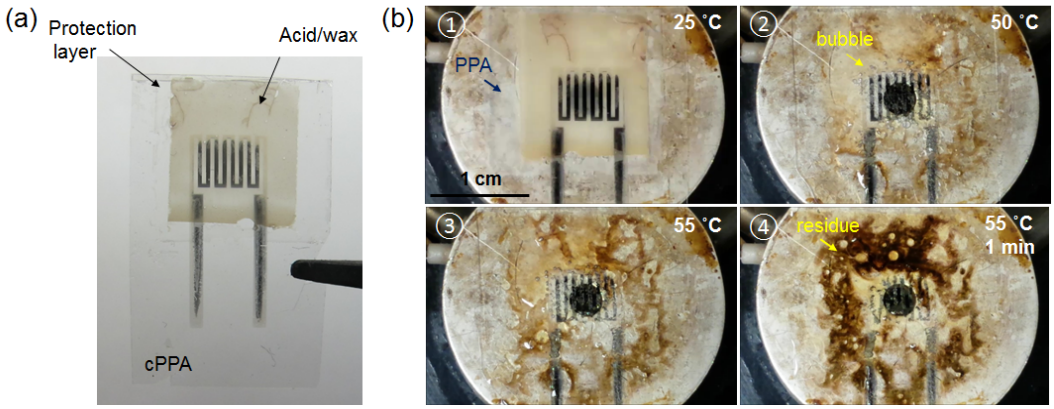

Figure 26. Heat-Activated Degradation of a Resistor on PPA Coated with Acid-Dispersed Silicone Wax Layer

(a) Free-standing Mg resistor on PPA with MSA-dispersed wax coating. (b) Thermally activated degradation of the resistor by acid, and degradation of Mg and PPA generates H_2 gas and blown residue, respectively.

Raman confocal imaging microscopy was used to characterize the PPA degraded by melting the MSA/wax coating. (Figure 25) The Raman spectrum of the residue was taken from a 32 µm PPA film with MSA/wax coating (100 µm thick coating contains 20 wt% MSA with 25 µm protection layer) after heating at 45 °C for 10 min. The carbonyl peak corresponding to the aldehyde monomer at 1680 cm^{-1} appeared in the spectrum of residue while the carbonyl peak was not present in the PPA spectrum. The spectral changes observed suggest that the use of MSA/wax coating with PPA successfully led to depolymerization reaction into monomer.

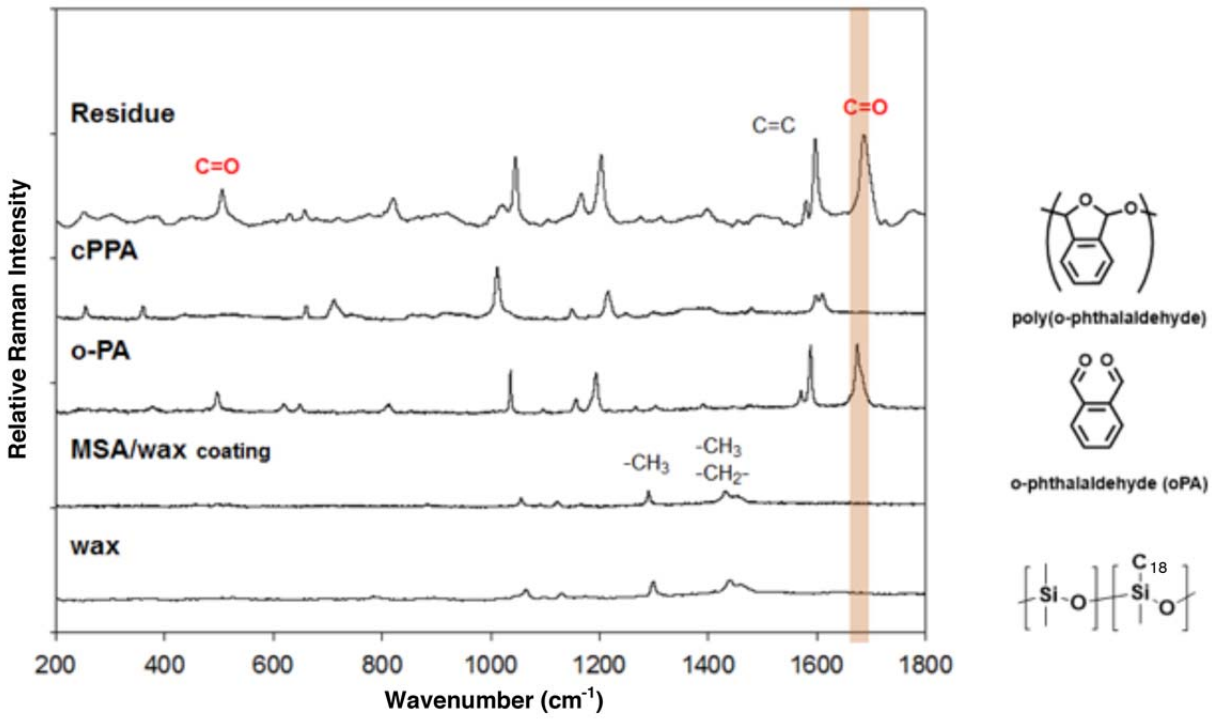

Figure 27. Raman Spectra of PPA Thermal Degradation Products, PPA, oPA and Coating

After degradation of PPA films by acid/wax coating at 45 °C for 10 min, Raman spectrum of the residue was compared to the spectra of PPA, o-PA monomer, MSA/wax coating and wax. The results show the formation C=O aldehyde stretch in the degradation products.

5 CONCLUSIONS

Metastable packaging materials were developed based on the acid-sensitive, depolymerizable poly(phthalaldehyde) (PPA), and thermally- and base-sensitive poly(olefin sulfone) (POS) polymers. Conditions for film preparation and fabrication of transient electronics on robust PPA and POS films were optimized. Three degradation triggers—direct activation by photoacid generation, thermal activation, and mechanical rupture of acid-filled microcapsules—were investigated.

For photo-triggered degradation of PPA, photoacid generators (PAGs) were incorporated into the film such that the acid generated upon UV exposure will disintegrate the polymer packaging. We successfully deposited silicon transistors, silicon diodes, and magnesium (Mg) resistors onto the PPA/PAG substrates. Using Mg resistors as a model system, two different PAGs were investigated, triphenylsulfonium triflate (TPST) and 2-(4-(4-methoxystyryl)-4,6-bis(trichloromethyl)-1,3,5-triazine (MBTT). It was found that TPST produced an acid that degraded only the polymer film while MBTT disintegrated both the substrate and the Mg/MgO electronic circuits. As one of the current challenges, the UV-activated MBTT does not erode electronics frabricated from silicon semiconductors albeit the PPA substrates were completely degraded. The transient behavior of PPA was monitored chemically by Fourier transform-infrared (FT-IR) spectroscopy and physically by dynamic mechanical analysis (DMA). Transience times were reduced by film processing conditions and complete disintegration of transient electronic packaging was achieved in under 1 hour.

In parallel, thermal triggers were investigated with thermally-unstable POS polymers and acid-containing wax capsules that release acid at elevated temperatures to degrade PPA films. Thermal triggering by radio frequency-induced heating was also explored as an alternative approach. Thermally triggering acid-containing capsules by heating the films at 55 °C released the acidic core contents, thereby degrading the PPA layer within 1 hour.

6 REFERENCES

1. Hwang, S.; Tao, H.; Kim, D.; Cheng, H.; Song, J.; Rill, E.; Brenckle, M.; Panilaitis, B.; Won, S.; Kim, Y.; Song, Y.; Yu, K.; Ameen, A.; Li, R.; Su, Y.; Yang, M.; Kaplan, D.; Zakin, M.; Slepian, M.; Huang, Y.; Omenetto, F.; Rogers, J. A. "A Physically Transient Form of Silicon Electronics." *Science* **2012**, *337*, 1640.

2. Kaitz, J. A.; Diesendruck, C. E.; Moore, J. S. "End group characterization of poly(phthalaldehyde): Surprising discovery of a reversible, cationic macrocyclization mechanism" *J. Am. Chem. Soc.* **2013**, *135*, 12755.

3. Jiang, Y.; Fréchet, J. M. J. "Design and synthesis of thermally labile polymers for microelectronics: poly(vinyl tert-butyl carbonate sulfone)," *Macromolecules* **1991**, *24*, 3528.

4. Caruso, M. M.; Blaiszik, B. J.; Jin, H.; Schelopf, S. R.; Stradley, D. S.; Sottos, N. R.; White, S. R.; Moore, J. S. "Robust, double-walled microcapsules for self-healing polymeric materials," *ACS Appl. Mater. Interfaces* **2010**, *2*, 1195.

LIST OF ACRONYMS, ABBREVIATIONS, AND SYMBOLS

ACRONYM	DESCRIPTION
A	amps
amu	atomic mass unit
BSA	benzenesulfonic acid
$CDCl_3$	chloroform-*d*
cm	centimeter
cm^{-1}	inverse centimeter (wavenumber units)
DBU	1,8-diazabicycloundec-7-ene
DSC	differential scanning calorimetry
e-beam	electron-beam
EPA	ethyl phenyl acetate
FT-IR	Fourier-transform infrared
GPC	gel-permeation chromatography
I_d	drain current
IR	infrared
kDa	kilodalton
mA	milliamps
MBTT	2-(4-(4-methoxystyryl)-4,6-bis(trichloromethyl)-1,3,5-triazine
Mg	magnesium
MgO	magnesium oxide
M_n	number-average molecular weight
m.p.	melting point
MSA	methanesulfonic acid
M_w	weight-average molecular weight
N-MOSFET	n-channel metal-oxide silicon field-effect transistors
NMR	nuclear magnetic resonance
*o*PA	*o*-phthalaldehyde
PAG	photoacid generator
PCyHS	poly(cyclohexene sulfone)
PDI	polydispersity index
PEG	poly(ethylene glycol)
PEO	poly(ethylene oxide)
PHS	poly(1-hexene sulfone)
PIN	p-i-n (p-type region/intrinsic region/n-type region)
PMBA	poly(*o*-(α-methyl)benzaldehyde
PMPS	poly(2-methyl-1-pentene sulfone)
POS	poly(olefin sulfone)
PPA	poly(phthalaldehyde)
PTFE	poly(tetrafluoroethylene)
PU/UF	poly(urethane)-poly(urea-formaldehyde)
PVA	poly(vinyl alcohol)
PVBCS	poly(vinyl *tert*-butyl carbonate sulfone)
R	resistance
rpm	revolution per minute
SEC	size-exclusion chromatography

ACRONYM	DESCRIPTION
SEM	scanning electron microscopy
SiNM	silicon nanomembrane
T_c	ceiling temperature
TGA	thermogravimetric analysis
TPST	triphenylsulfonium triflate
TsOH	toluenesulfonic acid
UV	ultra-violet
V_g	gate voltage
V	voltage
V	volt
wt%	weight percent
μm	micrometer
Ω	ohm
°C	degree in Celsius